Supporting Information

Constitutive modeling of strain-dependent bond breaking and healing kinetics of chemical Polyampholyte (PA) gel

Sairam Pamulaparthi Venkata[a,1#], Kunpeng Cui[b,1#], Jingyi Guo[a], Alan T. Zehnder[a], Jian Ping Gong[b,c,d], & Chung-Yuen Hui[a,c*]

[a] Field of Theoretical and Applied Mechanics, Department of Mechanical and Aerospace Engineering, Cornell University, Ithaca, New York, 14853, United States

[b] Institute for Chemical Reaction Design and Discovery (WPI-ICReDD), Hokkaido University, Sapporo 001-0021, Japan

[c] Soft Matter GI-CoRE, Hokkaido University, Sapporo 001-0021, Japan

[d] Faculty of Advanced Life Science, Hokkaido University, Sapporo 001-0021, Japan

[*] **Corresponding Author**, E-mail: ch45@cornell.edu (C.-Y.H.)

#These two authors contributed equally to this paper.

1. Discussion on healing rate and survivability function

Physically, the healing rate must increase with the number of broken bonds. The simplest assumption is that healing rate is directly proportional to the number of broken bonds divided by a characteristic healing time. This is a reasonable assumption since healing is achieved by ionic bonding to the number of available sites, so the reaction rate should be proportional to the number of broken bonds.

Eqn (1b) (main file) is based on the following physical reasoning. The rate of *decrease* of connected bonds N should increase with the number of connected bonds, that is,

$$-dN/dt \propto b(N), \qquad \text{(S1)}$$

where b is a monotonically increasing function of N. The function b can be inferred from a load relaxation test, since in our theory the healed bonds during a perfect relaxation test do not carry load. In a relaxation test, the amount of load relaxation is directly proportional to the number of broken bonds, this allows us to determine $N(t)$ and we found $b(N) \propto N^{\alpha_B}$. In our previous *PVA* gel system[1,2], experiments showed that the bond breaking kinetics is *insensitive* to the applied stretch, this means that the rate of change of the survivability function can be written as

$$-\frac{d\phi_B}{dt} = \frac{1}{t_B}\phi_B^{\alpha_B}. \qquad \text{(S2)}$$

However, for the PA gel system, we found that the bond breaking kinetics is sensitive to the stretch. Therefore, we modify eqn (S2) to reflect the effect of stretching on bond breaking. Using the affine approximation, we assume that the force acting on a chain is a function of first invariant of right Cauchy-Green tensor $I_1 = \mathbf{F}^T\mathbf{F}$, where $\mathbf{F}$ is the deformation tensor. As a result, the function b in eqn

---

[1] These authors contributed equally to this work. Numerical simulations are done by Sairam Pamulaparthi Venkata. Experimental data is provided by Kunpeng Cui.

(S1) also depends on I_1. We assume that b is separable, so for a chain formed at a time τ and survived until a time $t > \tau$, the rate of change of survivability function is

$$-\frac{d\phi_B}{dt} = \frac{1}{t_B}\phi^{\alpha_B} f\left[H(\tau,t)\right], \qquad H(\tau,t) = \text{trace}\left[\left(F^{\tau\to t}\right)^T F^{\tau\to t}\right]. \qquad \text{(S3)}$$

There is some similarity between our idea and Erying's theory [3](e.g. separability) which proposed that the bond dissociation rate has the form

$$-dN/dt \propto N\,exp\left(\frac{L_a\bar{F}}{k_BT}\right), \qquad \text{(S4)}$$

where L_a is the activation length for bond dissociation and $\bar{F}$ is the tensile force acting on a single polymer chain.

2. Steady state healing rate

From the second term in the R.H.S of eqn (2) (main file), we notice that the fraction of connected physical bonds at any time t is given by

$$\int_{-\infty}^{t} \phi_B(\tau,t,H^{\tau\to t})\chi(\tau)d\tau\,. \qquad \text{(S5a)}$$

By definition, the fraction of connected physical bonds *before the start of loading* ($t = 0$) is denoted by ρ. Here is it important to note that $H^{\tau\to 0} = 3$ since no loading occurs for time less than 0, that is, the deformation gradient is the identity tensor for time t < 0. In addition, for $t < 0$, the healing rate $\chi(t)$ is a constant given by its steady state value χ^{ss}, since the sample has rested for sufficiently long times so that the system is in dynamic equilibrium. Using eqn (S5a), we get

$$\begin{aligned}
\rho &= \int_{-\infty}^{0} \phi_B(\tau,t=0,H^{\tau\to 0})\chi(\tau)d\tau \\
&= \chi^{ss}\int_{-\infty}^{0}\left[1+\frac{\alpha_B-1}{t_B}\int_{\tau}^{0} f\left(H^{\tau\to 0}=3\right)ds\right]^{\frac{1}{1-\alpha_B}} d\tau, \qquad . \qquad \text{(S5b)} \\
&= \chi^{ss}\int_{-\infty}^{0}\left[1+\frac{\alpha_B-1}{t_B}(-\tau)\right]^{\frac{1}{1-\alpha_B}} d\tau = \frac{\chi^{ss}t_B}{2-\alpha_B}, \quad \forall\, 1<\alpha_B<2.
\end{aligned}$$

In the last step, we have used the fact that $f\left(H^{\tau\to 0}=3\right)=1$.

By setting $t = 0$ in the eqn (2) (main file) and eqn (1b) (main file) with $f = 1$ for $t \le 0$, we determine the steady state healing rate of physical bonds to be

$$\chi^{ss}t_H + 0 = \omega_{\text{phys}} - \chi^{ss}\frac{t_B}{2-\alpha_B}\left[\phi_B(0,0)\right]^{2-\alpha_B} \Rightarrow \chi^{ss} = \frac{\omega_{\text{phys}}}{t_H + \frac{t_B}{2-\alpha_B}}. \qquad \text{(S5c)}$$

3. Total strain energy

We assume that the polymer chains instantaneously relax as the bond breaks and carry zero stress. Also, the chains reattach in a relaxed state and carry no strain energy. By following a similar procedure as in our physical PA gel work[4] along with the addition of strain energy due to chemical bonds, we get the total strain energy $W(t)$ to be

$$\underbrace{W(t)}_{\text{Total strain energy}} = \underbrace{\omega_{\text{chem}} W_0(I_1(t))}_{\text{Strain energy due to chemical cross-links}} + \underbrace{\int_{-\infty}^{t} \phi_B(\tau,t)\chi(\tau) W_0\left[H(\tau,t)\right] d\tau}_{\text{Strain energy due to physical cross-links}}, \tag{S6}$$

$$I_1(t) = \text{trace}\left[\left(\mathbf{F}^{0\to t}\right)^T\left(\mathbf{F}^{0\to t}\right)\right].$$

4. Derivation of nominal stress from strain energy: Coleman-Noll Procedure

Following a similar procedure as in our previous works on PVA gel[1,2,5] and on physical PA gel[4], we briefly describe our procedure here. From eqn (S6), the total strain energy density $W(t)$ of the chemical PA gel system is given by

$$W(t) = \omega_{\text{chem}} W_0[I_1(t)] + \int_{-\infty}^{t} \chi(\tau)\phi_B(\tau,t,H(\tau,t)) W_0\left[H(\tau,t)\right] d\tau, \tag{S7}$$

Using eqn (S7) and $W_0\left[H(t,t)\right] = 0$, as $H(t,t) = 3$, we can calculate the change of strain energy density with respect to time as

$$\begin{aligned} \dot{W}(t) &\equiv \frac{dW(t)}{dt}, \\ &= \omega_{\text{chem}} \frac{d}{dt}\left(W_0\left[I_1(t)\right]\right) + \int_{-\infty}^{t} \chi(\tau)\phi_B(\tau,t,H(\tau,t)) \left.\frac{dW_0(I_1)}{dI_1}\right|_{I_1=H(\tau,t)} \frac{\partial H(\tau,t)}{\partial t} d\tau \\ &\quad + \int_{-\infty}^{t} \chi(\tau) \frac{\partial}{\partial t}\left(\phi_B(\tau,t,H(\tau,t))\right) W_0\left[H(\tau,t)\right] d\tau. \end{aligned} \tag{S8}$$

As in our physical PA gel work[4], the time derivative term of $H(\tau,t)$ in eqn (S8) can be written as

$$\frac{\partial H(\tau,t)}{\partial t} = \frac{\partial}{\partial t}\left(\text{trace}\left[\left(\mathbf{F}^{\tau\to t}\right)^T \mathbf{F}^{\tau\to t}\right]\right) = 2F_{ik}^{\tau\to t}\left(F_{jk}^{0\to\tau}\right)^{-1} \cdot \dot{F}_{ij}^{0\to t}. \tag{S9}$$

Also, we observe that the time derivative of survivability function does not contain time rate of change of deformation, $\dot{F}_{ij}^{0\to t}$. Terms associated with $\dot{\mathbf{F}}$ in eqn (S8) are equated with $\left[P_{ij} + p\left(F_{ji}^{0\to t}\right)^{-1}\right]\dot{F}_{ij}^{0\to t}$ in the energy balance equation to get

$$\begin{aligned} &\omega_{\text{chem}} \left.\frac{dW_0(I_1)}{dI_1}\right|_{I_1=I_1(t)} \frac{dI_1(t)}{dt} + \int_{-\infty}^{t} \chi(\tau)\phi_B(\tau,t,H(\tau,t)) \left.\frac{dW_0(I_1)}{dI_1}\right|_{I_1=H(\tau,t)} \frac{\partial H(\tau,t)}{\partial t} d\tau \\ &\qquad = \left[P_{ij} + p\left(F_{ji}^{0\to t}\right)^{-1}\right]\dot{F}_{ij}^{0\to t}. \end{aligned} \tag{S10}$$

where $\mathbf{P}$ is the first Piola-Kirchhoff stress tensor with p being the Lagrange multiplier enforcing incompressibility. Using eqns (S8)-(S10) we get

$$\left[P_{ij}+p\left(F_{ji}^{0\to t}\right)^{-1}\right]\dot{F}_{ij}^{0\to t}=\omega_{\text{chem}}\left.\frac{dW_0(I_1)}{dI_1}\right|_{I_1=I_1(t)}2F_{ij}^{0\to t}\dot{F}_{ij}^{0\to t}+\int_{-\infty}^{t}\chi(\tau)\phi_B(\tau,t,H(\tau,t))\left.\frac{dW_0(I_1)}{dI_1}\right|_{I_1=H(\tau,t)}2F_{ik}^{\tau\to t}\left(F_{jk}^{0\to\tau}\right)^{-1}\cdot\dot{F}_{ij}^{0\to t}d\tau. \tag{S11a}$$

and

$$P_{ij}=-p\left(F_{ji}^{0\to t}\right)^{-1}+\omega_{\text{chem}}\left.\frac{dW_0(I_1)}{dI_1}\right|_{I_1=I_1(t)}2F_{ij}^{0\to t}+\int_{-\infty}^{0}\chi^{ss}\phi_B(\tau,t,H(\tau,t))2\left.\frac{dW_0(I_1)}{dI_1}\right|_{I_1(t)}F_{ij}^{0\to t}d\tau+\int_{0}^{t}\chi(\tau)\phi_B(\tau,t,H(\tau,t))2\left.\frac{dW_0(I_1)}{dI_1}\right|_{I_1=H(\tau,t)}F_{ik}^{\tau\to t}\left(F_{jk}^{0\to\tau}\right)^{-1}d\tau. \tag{S11b}$$

The nominal stress in eqn (S7b) can re-written in tensor notation as

$$\mathbf{P}(t)=-p\left(\mathbf{F}^{0\to t}\right)^{-T}+\omega_{\text{chem}}2\left.\frac{dW_0}{dI_1}\right|_{I_1(t)}\mathbf{F}^{0\to t}+\left\{\chi^{ss}\frac{t_B}{2-\alpha_B}\left[\phi_B\left(0,t,I_1(t)\right)\right]^{2-\alpha_B}\right\}2\left.\frac{dW_0}{dI_1}\right|_{I_1(t)}\mathbf{F}^{0\to t}+\int_{0}^{t}\phi_B(\tau,t,H(\tau,t))\chi(\tau)2\left.\frac{dW_0}{dI_1}\right|_{I_1=H(\tau,t)}\mathbf{F}^{\tau\to t}\left(\mathbf{F}^{0\to\tau}\right)^{-T}d\tau. \tag{S12}$$

4.1. Nominal stress in Uniaxial Tension test

Let the nominal stretch at any given time t be $\lambda(t)$. Now the deformation gradient tensor becomes

$$\boldsymbol{F}^{0\to t}=\begin{bmatrix}\lambda(t) & 0 & 0\\ 0 & 1/\sqrt{\lambda(t)} & 0\\ 0 & 0 & 1/\sqrt{\lambda(t)}\end{bmatrix},\quad \text{with } \det\mathbf{F}=1. \tag{S13}$$

Substituting eqn (S13) in eqn (S12) and using $P_{22}=0$ to determine *p,* the nominal stress under uniaxial tension loading is

$$\begin{aligned}P_{11}(t)\equiv P(t)&=\left[\omega_{\text{chem}}+\chi^{ss}\int_{-\infty}^{0}\phi\left(\tau,t,H^{\tau\to t}\right)d\tau\right]2\left.\frac{dW_0}{dI_1}\right|_{I_1(t)}\left(\lambda(t)-\lambda(t)^{-2}\right)\\&+\int_{0}^{t}\left[\chi(\tau)\phi\left(\tau,t,H^{\tau\to t}\right)2\left.\frac{dW_0}{dI_1}\right|_{H^{\tau\to t}}\left[\frac{\lambda(t)}{\lambda^2(\tau)}-\frac{\lambda(\tau)}{\lambda^2(t)}\right]\right]d\tau,\\&=\left[\omega_{\text{chem}}+\chi^{ss}\frac{t_B}{2-\alpha_B}\left[\phi\left(\tau=0,t,H^{0\to t}\right)\right]^{2-\alpha_B}\right]2\left.\frac{dW_0}{dI_1}\right|_{I_1(t)}\left(\lambda(t)-\lambda(t)^{-2}\right)\\&+\int_{0}^{t}\left[\chi(\tau)\phi\left(\tau,t,H^{\tau\to t}\right)2\left.\frac{dW_0}{dI_1}\right|_{H^{\tau\to t}}\left[\frac{\lambda(t)}{\lambda^2(\tau)}-\frac{\lambda(\tau)}{\lambda^2(t)}\right]\right]d\tau.\end{aligned} \tag{S14}$$

4.2. Nominal stress in Tensile-Relaxation test

In an actual experiment, it takes a finite loading time t_1 before we achieve the desired nominal stretch ratio λ_0. Once the desired stretch ratio is reached it is held constant to start the relaxation test.

The nominal stress in the loading direction is given by

$$P(t)=\begin{cases}\left[\omega_{\text{chem}}+\chi^{ss}\dfrac{t_B}{2-\alpha_B}\left[\phi\left(\tau=0,t,H^{0\to t}\right)\right]^{2-\alpha_B}\right]2\dfrac{dW_0}{dI_1}\Big|_{I_1(t)}\left(\lambda(t)-\lambda(t)^{-2}\right) & \text{if } t\le t_1\\ +\displaystyle\int_0^t\left[\chi(\tau)\phi\left(\tau,t,H^{\tau\to t}\right)2\frac{dW_0}{dI_1}\Big|_{I_1=H^{\tau\to t}}\left[\frac{\lambda(t)}{\lambda^2(\tau)}-\frac{\lambda(\tau)}{\lambda^2(t)}\right]\right], & \\ \left[\omega_{\text{chem}}+\chi^{ss}\dfrac{t_B}{2-\alpha_B}\left[\phi\left(\tau=0,t,H^{0\to t}\right)\right]^{2-\alpha_B}\right]2\dfrac{dW_0}{dI_1}\Big|_{I_1(t)}\left(\lambda_0-\lambda_0^{-2}\right) & \text{if } t>t_1\\ +\displaystyle\int_0^{t_1}\left[\chi(\tau)\phi\left(\tau,t,H^{\tau\to t}\right)2\frac{dW_0}{dI_1}\Big|_{I_1=H^{\tau\to t}}\left[\frac{\lambda_0}{\lambda^2(\tau)}-\frac{\lambda(\tau)}{\lambda_0^2}\right]\right]. & \end{cases} \quad \text{(S15)}$$

5. Material parameter estimates from experiments

5.1. Estimate for small strain instantaneous shear modulus

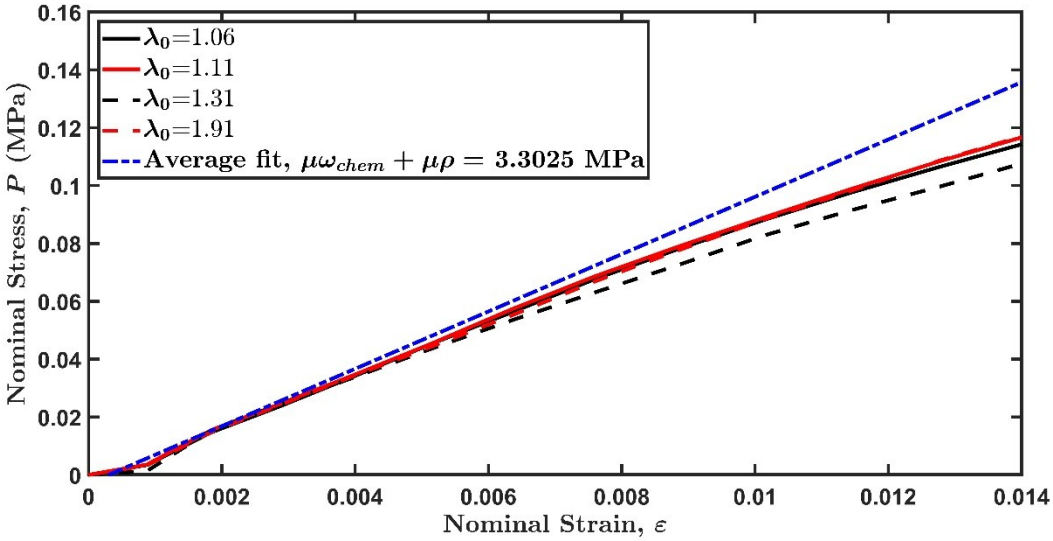

Fig. S1. Fitting the initial slope from the loading portion of four tensile-relaxation tests carried out at four stretch ratios λ_0 (solid lines). The experimental nominal stress – nominal strain plots shown here are from the same data set. We observe that all the four relaxation tests fall on the same line at small strains (less than 0.5%).

The nominal stress in a uniaxial tension test is given by eqn (S14). As the loading begins, at small times and small strains, there are very few newly formed bonds and the fraction of physical bonds connected in the material are almost same as their steady state fraction ρ. This results in integral term in the eqn (S14) to be small in comparison with the first term. As strains are small at short times, we can neglect the strain hardening $\left(2\dfrac{dW_0}{dI_1}\Big|_{I_1(t)}\approx\mu\right)$ and strain dependent breaking terms to get

$$P_{11}\left(t\to 0^{+}\right)\approx \mu\left(\omega_{\text{chem}}+\chi^{ss}\frac{t_B}{2-\alpha_B}\right)\left(\lambda\left(t\to 0^{+}\right)-\lambda\left(t\to 0^{+}\right)^{-2}\right)$$
$$\approx 3\mu\left(\omega_{\text{chem}}+\chi^{ss}\frac{t_B}{2-\alpha_B}\right)\varepsilon = 3\mu\left(\omega_{\text{chem}}+\rho\right)\varepsilon = E_0\varepsilon \quad , \qquad \text{(S16)}$$

where E_0 is the instantaneous Young's modulus which represents the initial slope of the nominal stress – nominal strain curve. This allows us to use the initial slope from the loading portion of tensile-relaxation test to determine $\mu\left(\omega_{\text{chem}}+\rho\right)$ as shown in Fig. S1. We notice the small strain instantaneous shear modulus to be $\mu\left(\omega_{\text{chem}}+\rho\right)\approx 3.30$ MPa (1/3 of the slope of the dotted blue line) from Fig. S1.

5.2. Estimate for critical stretch ratio λ_c

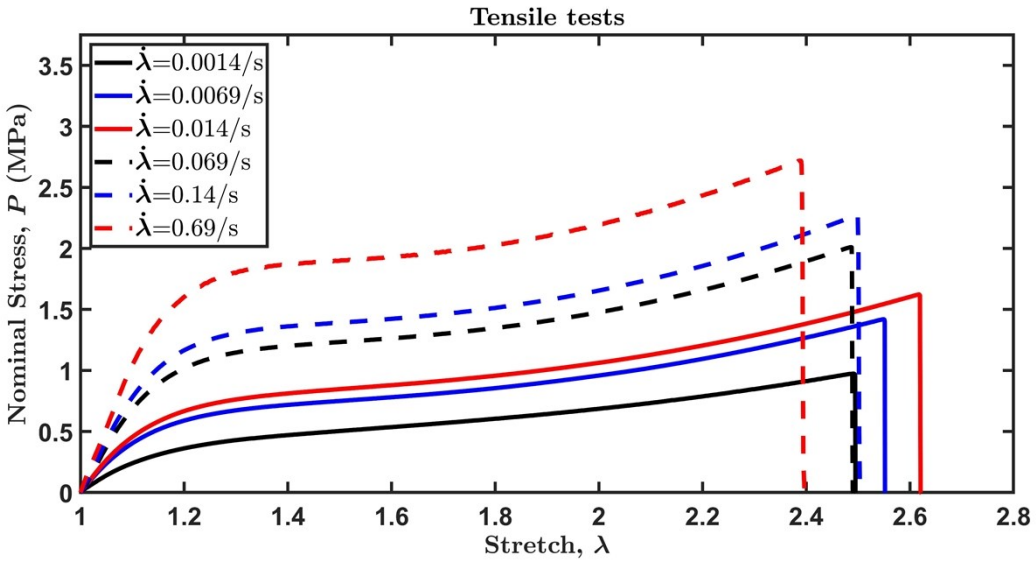

Fig. S2. Uniaxial tension test data for chemical PA-gel for different stretch rates.

Uniaxial tension test data in Fig. S2 shows that the slope of nominal stress versus nominal strain plots decrease rapidly around a critical strain of $\lambda_c \in (1.2, 1.3)$ for different loading rates. This critical strain was associated with "yielding" in the double network gel[6]. Also, the "yield" stress increases with increasing strain rate, but the yield strain remains almost the same. This observation is consistent with our assumption that the breaking kinetics in eqn (1b) (main file) is controlled by the stretch/strain experienced by the bond.

6. Data sets used for optimization process

As in our physical PA gel work[4], we follow a similar procedure here. The data used for optimization process from simple tension, tensile-relaxation, and cyclic tests is shown in Fig. S3. Here, solid black lines represent the experimental data and blue dotted lines represent the optimization points. The objective function is to minimize the least squares error in nominal stress predicted by our model (see eqn (S17)) at these optimization points. In Fig. S3, for brevity, LR and UR are used to represent loading and unloading rates respectively. To capture the change in curvature of nominal stress with nominal strain accurately, more weightage is given to the curved regions by selecting relatively more optimization points around these regions. We use a *lsqcurvefit* inbuilt function with *trust-region-reflective* algorithm in *MATLAB 2018a* version for the optimization process.

$$\sum_i \left(\mathsf{F}\left(\boldsymbol{\eta}, xdata_i\right) - ydata_i\right)^2, \quad lb \le \boldsymbol{\eta} \le ub, \qquad \text{(S17)}$$

where $\boldsymbol{\eta}$ denotes a vector of nine material parameters in Table 1 (main file) and F refers to the nominal stress predicted by our model under different loading histories (simple tension, tensile-relaxation, and cyclic tests). Here, *xdata* is a column vector of selected nominal stretch values in simple tension and cyclic tests, and a column vector of selected time points in tensile-relaxation tests. Whereas *ydata* is the experimental nominal stress values at these corresponding *xdata* points. The *lb* and *ub* denote lower and upper bonds on $\boldsymbol{\eta}$ respectively.

For the optimization process to be computationally efficient and less time consuming, we replace the history dependent reattachment rate $(\chi(t))$ with the steady state value (χ^{ss}). This assumption helps us avoid solving the integral equation (eqn (2), main file). Now, as a part of optimization process, we obtain multiple local optimum sets with less than 10 percent relative error between model prediction and experiments at any optimization point. So, we use estimates from Section S5 to select an optimal parameter set from these multiple optimums.

Now, with this chosen parameter set and by solving the integral equation, we recalculate $\mathsf{F}\left(\boldsymbol{\eta}, xdata_i\right)$ to check if $\left|\mathsf{F}\left(\boldsymbol{\eta}, xdata_i\right) - ydata_i\right| \le 0.1\left|ydata_i\right| \ \forall\ i$ and slightly fine tune the parameter set to get the best possible fits.

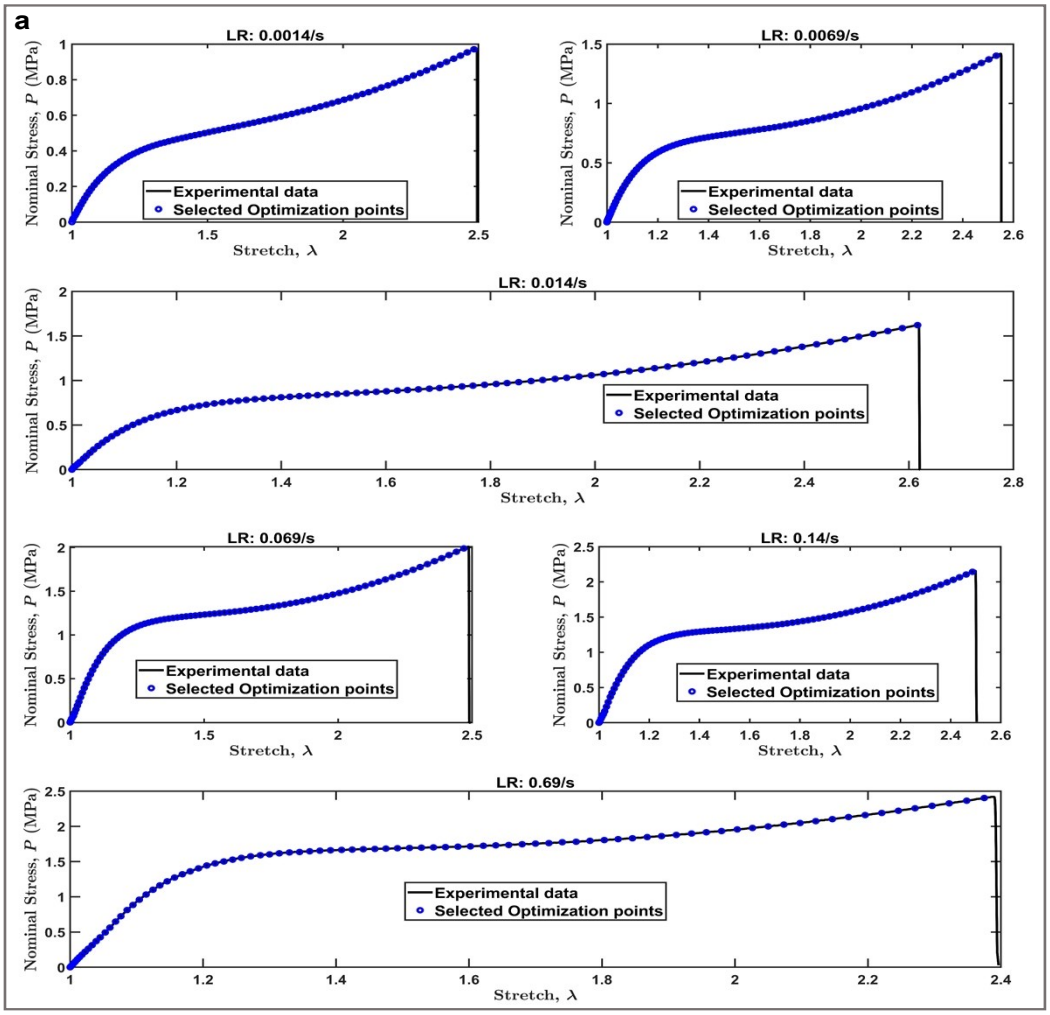

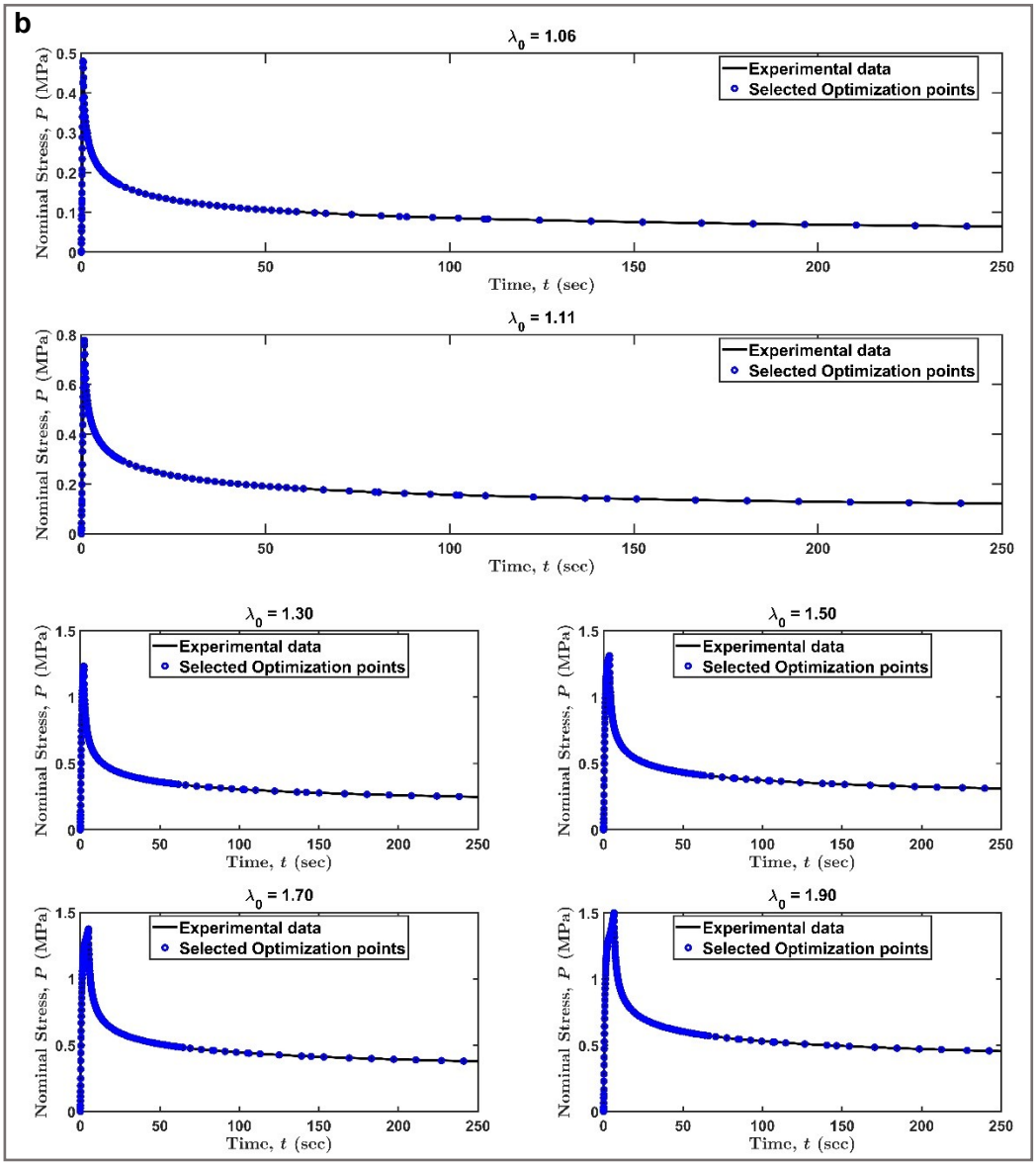
b
λ_0 = 1.06
Experimental data
Selected Optimization points
Nominal Stress, P (MPa)
Time, t (sec)
λ_0 = 1.11
Experimental data
Selected Optimization points
Nominal Stress, P (MPa)
Time, t (sec)
λ_0 = 1.30
Experimental data
Selected Optimization points
Nominal Stress, P (MPa)
Time, t (sec)
λ_0 = 1.50
Experimental data
Selected Optimization points
Nominal Stress, P (MPa)
Time, t (sec)
λ_0 = 1.70
Experimental data
Selected Optimization points
Nominal Stress, P (MPa)
Time, t (sec)
λ_0 = 1.90
Experimental data
Selected Optimization points
Nominal Stress, P (MPa)
Time, t (sec)

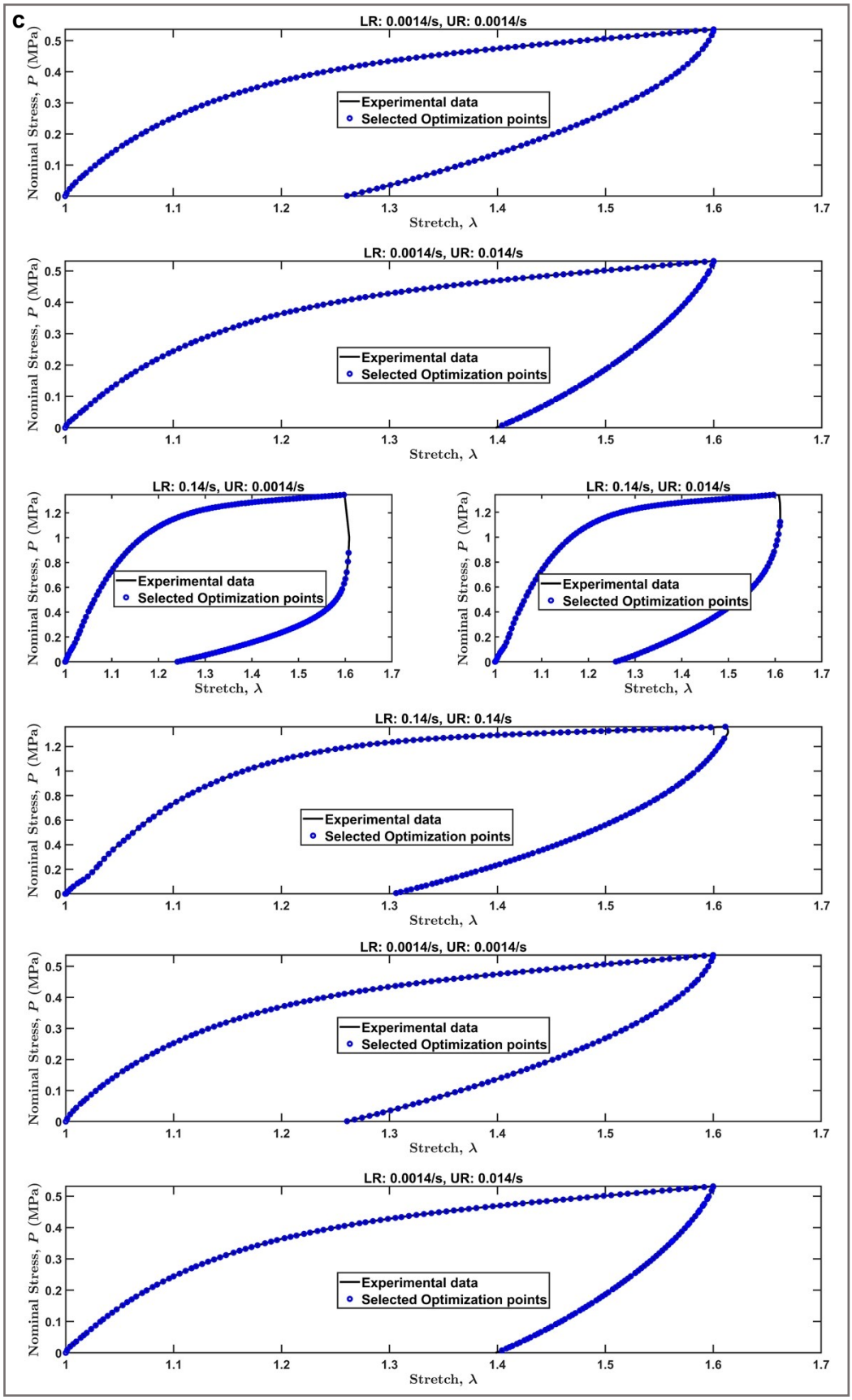

Fig. S3. We present all the representative data sets used for optimization process here (a) simple tension, (b) tensile-relaxation tests, and (c) loading-unloading tests which are used for least squares optimization

process are presented here. All the 9 independent material parameters in Table 1 (main file) are optimized to get the minimum least squares error in nominal stress at the selected optimization points (shown as blue dotted circles) from all the curves shown here. Here, LR represents loading rate and UR represents unloading rate.

7. Exponential of power law form of breaking function and results

As mentioned in the main file (Section 6), here we use an accelerating breaking function of form $f(I_1)=\exp\left\{\left(1+\frac{I_1-3}{I_c-3}\right)^m-1\right\}$, $I_c=\lambda_c^2+\frac{2}{\lambda_c}$ as in our previous work[4] and observe almost as good fits as in the results presented in the main file (Section 5). The material parameters for the model with f of exponential of power law form are mentioned in the Table S1.

Table S1: The material parameters required for constitutive model are listed below.

Strain dependent parameters			
$\alpha_B=1.8023$	$t_B=0.1169\,\text{sec}$	$t_H=0.01\,\text{sec}$	$\omega_{\text{phys}}=0.99$
Strain dependent accelerated breaking function parameters, f			
$m=0.5452$		$\lambda_c=1.0854$	
Undamaged network strain energy density function, Yeoh's model, W_0			
$c_1\equiv\mu/2=1.8500\,\text{MPa}$	$c_2/c_1=0.2968$	$c_3/c_1=0.1566$	
Derived material parameters			
$\rho=0.9735$ **(see eqn (3a), main file)**	$\chi^{SS}=1.6466\,s^{-1}$ **(see eqn (3b), main file)**	$\mu(\omega_{\text{chem}}+\rho)\equiv\frac{E_0}{3}=3.6390\,\text{MPa}$	

Using the material parameters from Table S1, the following numerical results are computed.

7.1. Cyclic tests

7.1.1. Small strain

The uniaxial cyclic tests for two different loading and unloading rates are presented in the Fig. S4. In comparison to the Fig. 1 (main file), the model with f of power law form fits the loading part slightly better for both the loading-unloading histories in small strain regime (see Fig. S4).

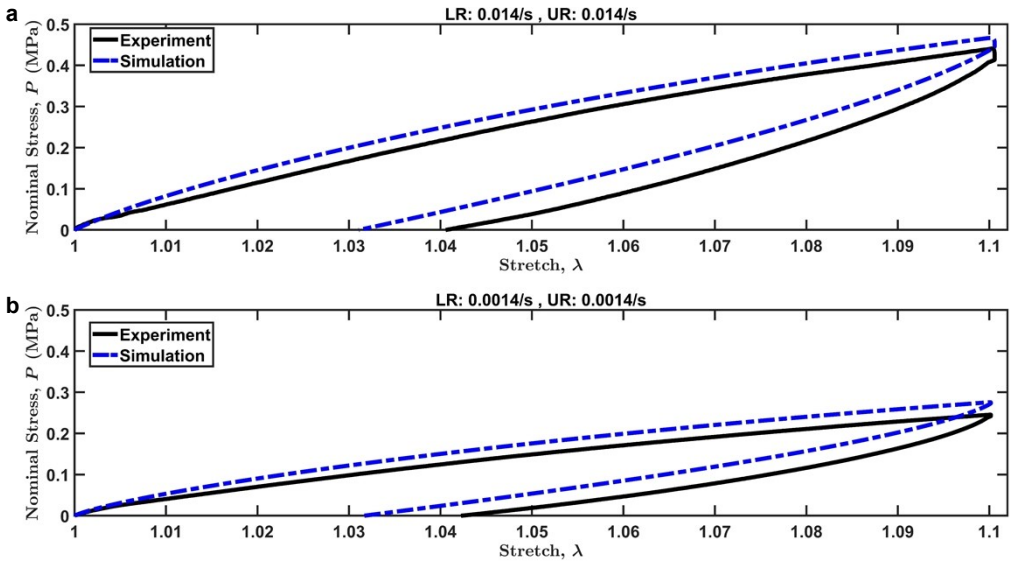

Fig. S4. Nominal stress P (MPa) vs nominal stretch λ for loading and unloading tests with two different strain rates are shown here. (a) The upper plot has a loading rate (LR) and unloading rate (UR) of 0.014/s each. (b) The lower plot has a loading rate (LR) and unloading rate (UR) of 0.0014/s each. Solid black lines represent the experiment data and our simulation results using parameters in Table S1 are shown as dash-dotted blue lines.

7.1.2. Large strain

We observe the nominal stress fits for cyclic tests under large strain using f with exponential of power law form (see Fig. S5) or power law form (see Fig. 2, main file) are both in good agreement with experiments.

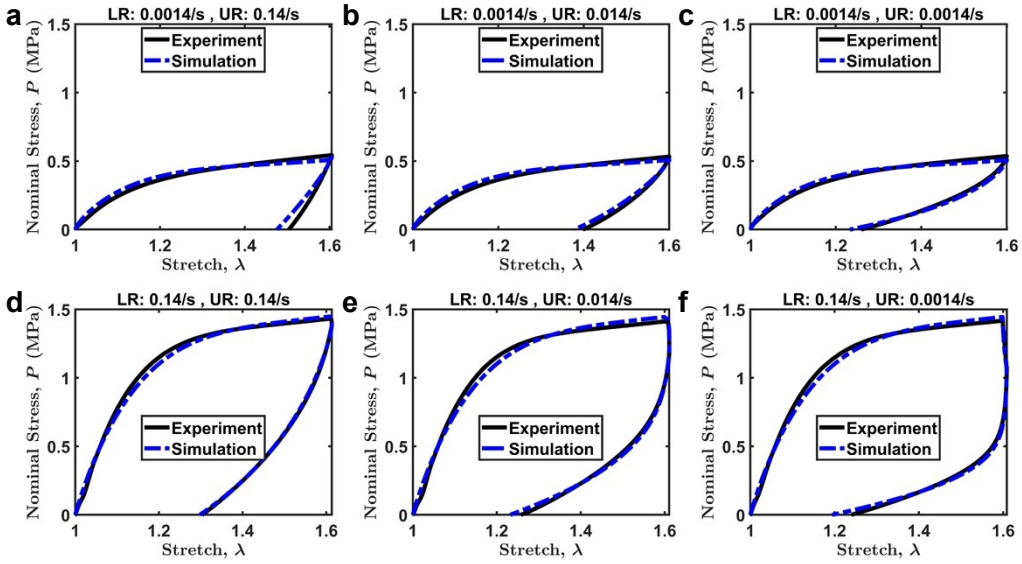

Fig. S5. Nominal stress P (MPa) vs nominal stretch λ for loading and unloading tests with different strain rates are shown here. (a), (b), and (c): The upper plots have a loading rate (LR) of 0.14/s and unloading rates (UR) of 0.14/s, 0.014/s, and 0.0014/s from left to right respectively. (d), (e), and (f): Similarly, the lower plots have a loading rate of 0.0014/s and unloading rates of 0.14/s, 0.014/s, and 0.0014/s from left to right respectively. Solid black lines represent the experiment data and our simulation results using parameters in Table S1 are shown as dash-dotted blue lines.

7.2. Tensile-Relaxation tests

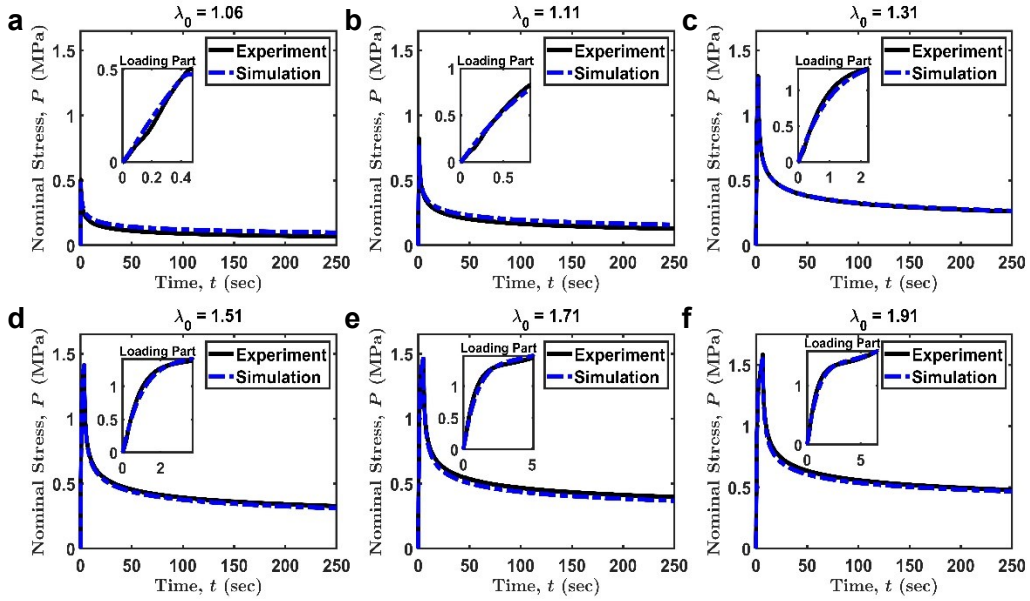

Fig. S6. Nominal stress P (MPa) vs time t (sec) for tensile-relaxation tests with different nominal stretch ratios are shown here. Solid black lines represent the experiment data and our simulation results using parameters in Table S1 are shown as dash-dotted blue lines. Loading part of the tests are shown as insets. Relaxation tests are carried out at six stretch ratios (a) $\lambda_0 = 1.06$, (b) $\lambda_0 = 1.11$, (c) $\lambda_0 = 1.31$, (d) $\lambda_0 = 1.51$, (e) $\lambda_0 = 1.71$, and (f) $\lambda_0 = 1.91$.

From Fig. S6 and Fig. 3 (main file), we observe that predictions from both the models are in good agreement with the tensile-relaxation tests.

7.3. Simple Tension

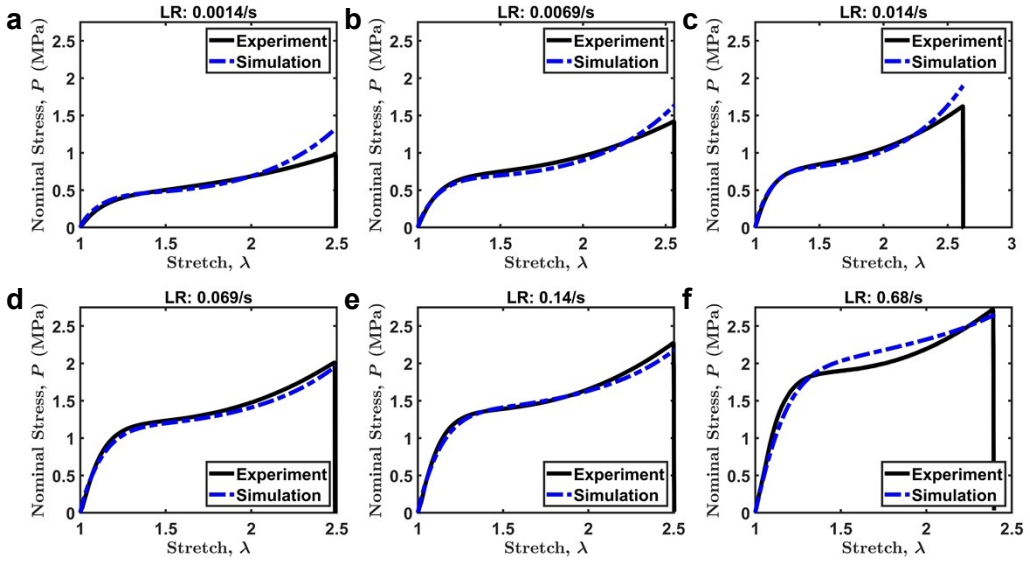

Fig. S7. Nominal stress P (MPa) vs nominal stretch λ for simple tension tests with six loading rates (LR) are presented here. (a) 0.0014/s, (b) 0.0069/s, (c) 0.014/s, (d) 0.069/s, (e) 0.14/s, and (f) 0.68/s.

Solid black lines represent the experiment data and our simulation results using parameters in Table S1 are shown as dash-dotted blue lines.

By comparing Fig. S7 with Fig. 4 (main file), we observe that the model with acceleration breaking function f of power law form fits the tensile tests slightly better for loading rates 0.0014/s-0.014/s. But the general behavior captured by both the models is almost similar.

7.4. Load bearing characteristics of physical and chemical bonds

From Fig. S8 and Fig. 5 (main file), we notice that for both the models, the stress carried by both physical and chemical bonds for different loading histories are almost similar. This is because the behavior of accelerating breaking function f from both the models is almost the same (see, Fig. S9). So, the rate at which the physical bonds break is also similar, as characteristic breaking time t_B and rate of decay of survivability function α_B are close enough in both these models (see Table S1 and Table 1, main file). This leads to similar loading bearing characteristics in both these models.

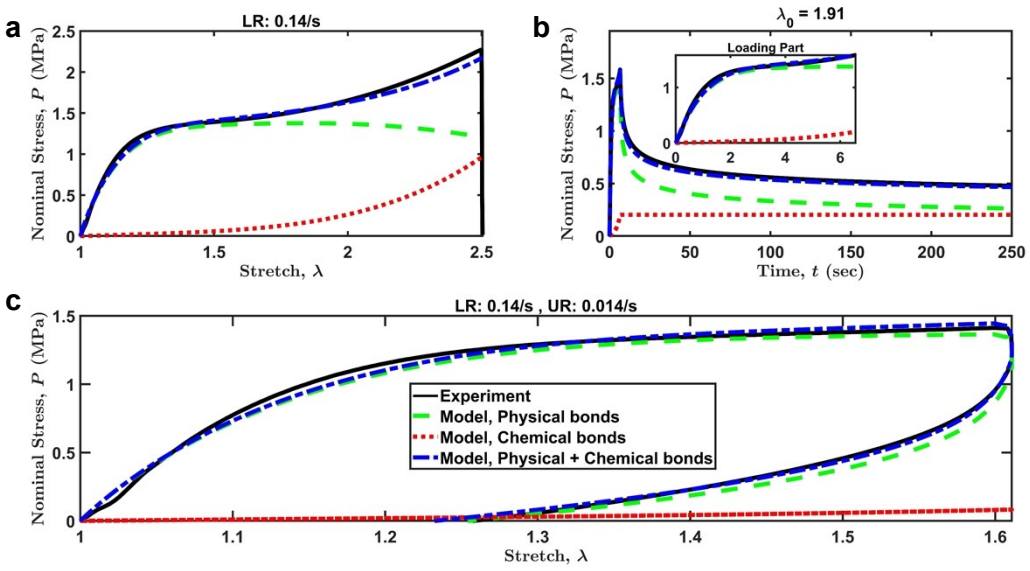

Fig. S8. For different loading histories, stress contributions from both physical and chemical bonds are computed using our model. (a) simple tension, (b) tensile-relaxation, and (c) cyclic test. The tensile test is carried out using a loading rate (LR) of 0.14/s. The stretch ratio in the tensile-relaxation test is $\lambda_0 \approx 1.91$. The cyclic test has a loading rate (LR) of 0.14/s and an unloading rate (UR) of 0.014/s. Solid black lines represent the experiment data, the stress contribution from physical bonds is shown in green dotted lines, the stress contribution from chemical bonds is shown in red dotted lines, and total stress contribution from both physical and chemical bonds is represented by blue dash-dotted lines.

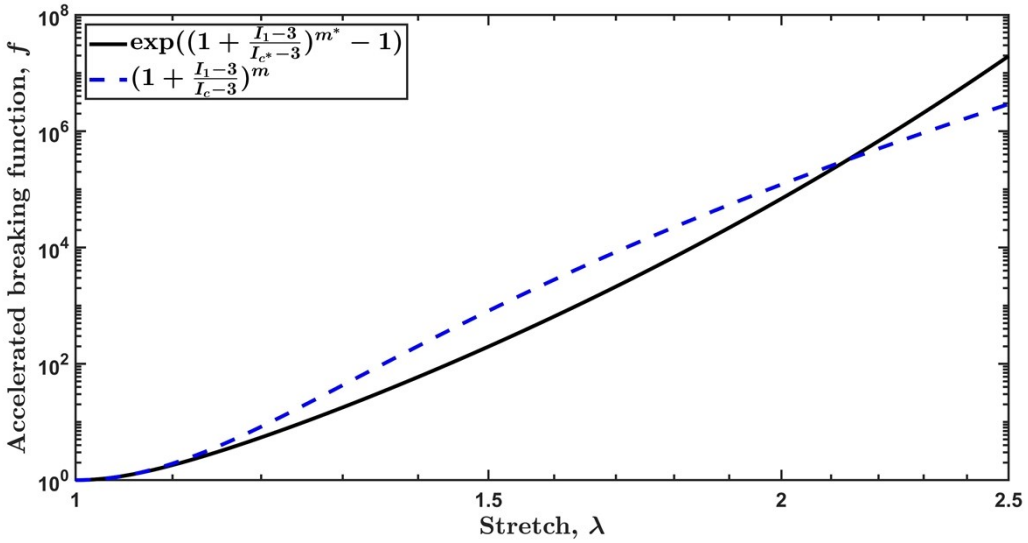

Fig. S9. Behavior of accelerating breaking function f for two different models. The values of material parameters I_c^* and m^* are same as I_c and m in Table S1. The values of material parameters I_c and m in power law form model are same as the ones in the Table 1 (main file).

Next, we observe the behavior of time dependent healing rate.

Fig. S10 plots show that the behavior of healing rate of physical bonds for this model is almost similar to the ones presented in the Fig. 6 (main file). We observe healing rates for the accelerating breaking function of power law form model (See Fig. 6, main file) to be slightly higher when compared to the exponential of power law form model (See Fig. S10) under different loading histories. On a general note, healing rate increases during the loading part and decreases continuously during the relaxation part.

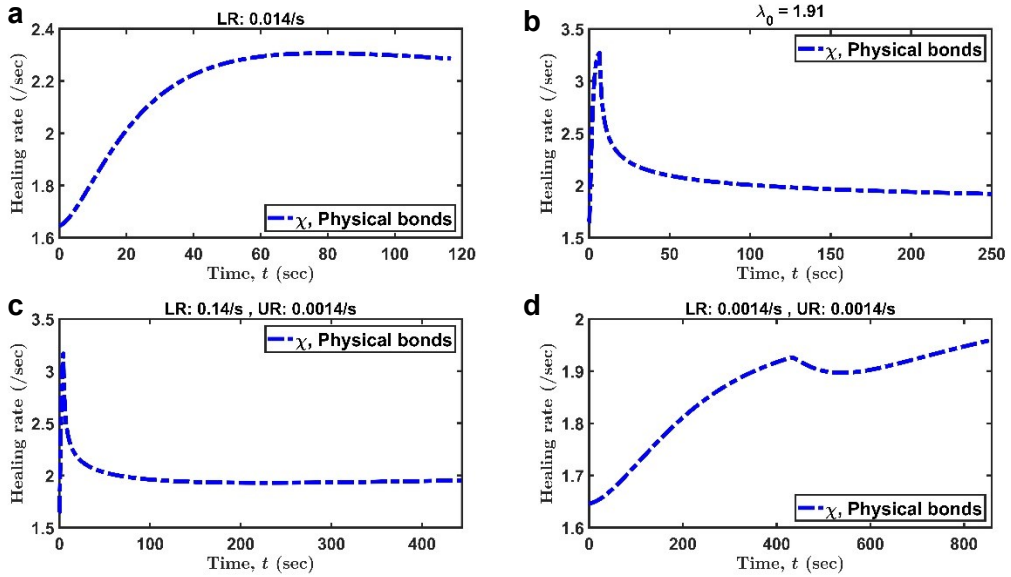

Fig. S10. Healing rate ($\chi(t)$) (in /s) for physical bonds (blue dash-dotted lines) vs time (s) for three types of mechanical testing are shown here. (a) The top left plot is a simple tension test for a loading rate (LR) of 0.014/s. (b) The top right plot is a tensile-relaxation test with a desired nominal stretch ratio

of $\lambda_0 \approx 1.91$. (c) and (d) The two lower plots are cyclic tests with a loading-unloading rates (LR-UR) of 0.14/s-0.0014/s and 0.0014/s-0.0014/s.

References

1 R. Long, K. Mayumi, C. Creton, T. Narita and C.-Y. Hui, *Macromolecules*, 2014, **47**, 7243–7250.
2 J. Guo, R. Long, K. Mayumi and C.-Y. Hui, *Macromolecules*, 2016, **49**, 3497–3507.
3 A. Tobolsky and H. Eyring, *J. Chem. Phys.*, 1943, **11**, 125–134.
4 S. P. Venkata, K. Cui, J. Guo, A. T. Zehnder, J. P. Gong and C.-Y. Hui, *Extreme Mech. Lett.*, 2021, **43**, 101184.
5 R. Long, K. Mayumi, C. Creton, T. Narita and C.-Y. Hui, *J. Rheol.*, 2015, **59**, 643–665.
6 T. Matsuda, T. Nakajima, Y. Fukuda, W. Hong, T. Sakai, T. Kurokawa, U. Chung and J. P. Gong, *Macromolecules*, 2016, **49**, 1865–1872.